Dyes and Pigments 99 (2013) 185–191

Contents lists available at SciVerse ScienceDirect

Dyes and Pigments

journal homepage: www.elsevier.com/locate/dyepig

# Synthesis and antifungal photodynamic activities of a series of novel zinc(II) phthalocyanines substituted with piperazinyl moieties

Bi-Yuan Zheng, Hong-Peng Zhang, Mei-Rong Ke, Jian-Dong Huang*

*College of Chemistry and Chemical Engineering, Fuzhou University, Fuzhou 350108, China*

ARTICLE INFO

*Article history:*
Received 1 March 2013
Received in revised form
24 April 2013
Accepted 25 April 2013
Available online 9 May 2013

*Keywords:*
Zinc(II) phthalocyanine
Photosensitizer
Photodynamic therapy
Single oxygen
Antifungal
*Candida albicans*

ABSTRACT

A series of novel zinc(II) phthalocyanines tetra-substituted or mono-substituted with piperazinyl moieties linked by different ethoxy chains has been prepared and characterized. The effects of the *N*-protecting group of piperazinyl moiety, length of ethoxy chains and number of substitutes on the photophysical, photochemical properties, cellular uptakes and in vitro photodynamic antifungal activities have also been examined. All of these compounds are essentially non-aggregated and good singlet oxygen generators with quantum yields ($\Phi_\Delta$) of 0.54–0.77 in *N*,*N*-dimethylformamide. The photodynamic activity of these compounds against *Candida albicans* follows the order: **7** > **5a** > **5b** > **4a** ≈ **4b**. The mono-substituted phthalocyanine **7** exhibits the highest photodynamic inactivation of *C. albicans* with an $IC_{90}$ value of 9 μM, which can be attributed to its better amphiphilicity and even higher cellular uptake. The results suggest that phthalocyanine **7** is a potential photosensitizer for antifungal photodynamic therapy.



## 1. Introduction

Photodynamic therapy (PDT) is a minimally invasive method that employs a photosensitizer molecule, which produces reactive oxygen species (ROS) to cause cell and tissue damage by exposure to lights with a specific wavelength [1]. It is a well-recognized therapeutic modality for a variety of premalignant and malignant diseases [2–4]. Recently, PDT utilized for the treatment of pathogenic fungi has received considerable interest as a result of the emergence of antibiotic-resistant mycoses and the increase of fungal infections [5–10]. As a promising therapeutic approach, antifungal PDT, which inactivates the pathogenic microorganisms by ROS generated by photosensitizers, presents several advantages, such as broad spectrum of action, high therapeutic efficacy which is independent of the antibiotic resistance pattern of the given microbial strain, and limited damage to the host tissue, in contrast to the typical antibiotic therapeutics [5–10].

*Candida albicans* is the most common fungal pathogen that can cause both superficial and systemic infections. Owing to the augmented numbers of immunocompromised or hospitalized patients who suffer from cancer or AIDS, the infections associated with *C. albicans* have increased dramatically in last decades [11–13]. Moreover, the resistance of *C. albicans* against traditional antifungal agents, such as fluconazole, is increasing year by year [14,15]. PDT has been employed to inactivate *C. albicans* and the antifungal effects of several kinds of photosensitizers (such as phenothiazine dyes, porphyrins, and 5-aminolevulinic acid) have been briefly reported [12,13,16–19].

Phthalocyanines have found to be highly promising as second-generation photosensitizers for PDT owing to their desirable photophysical and photochemical properties [20,21]. However, the photodynamic activities toward fungi remain little studied for phthalocyanine-based photosensitizers [22–27]. In order to rationally design the phthalocyanines especially for the photodynamic treatment of fungi, it is necessary to carefully explore the structure–activity relationships via variedly functionalized phthalocyanines. Very recently, our group has investigated the photodynamic activities against *C. albicans* of a series of silicon(IV) phthalocyanines axially substituted with different functional groups, and discussed the effect of axial substituents [27]. The results from our [27] and other groups [23,24] suggest that the photosensitizers bearing cationic or protonable groups such as tertiary amines generally show higher photocytotoxicities against pathogenic microorganisms compared with the neutral and anionic analogs. As an extension of our work, we report herein a series of novel zinc(II) phthalocyanines tetra-substituted or mono-substituted with piperazinyl moieties linked by different ethoxy chains. The synthesis, photophysical and

* Corresponding author. Tel.: +86 591 22866235; fax: +86 591 22866227.
*E-mail addresses:* jdhuang@fzu.edu.cn, 13805009843@163.com (J.-D. Huang).

0143-7208/$ – see front matter © 2013 Elsevier Ltd. All rights reserved.
http://dx.doi.org/10.1016/j.dyepig.2013.04.032

photochemical properties, cellular uptakes and in vitro photodynamic activities against *C. albicans* of these compounds are described in this paper. The effects of the *N*-protecting group of piperazinyl moiety, length of ethoxy chains and number of substitutes on the physicochemical properties and antifungal activities have also been discussed.

## 2. Experimental

### 2.1. General

All the reactions were performed under an atmosphere of nitrogen. *N*,*N*-dimethylformamide (DMF) and *n*-pentanol were dried over molecular sieves and further distilled under reduced pressure before use. Potassium carbonate was activated by muffle at 300 °C under normal pressure. Cremophor EL and unsubstituted zinc(II) phthalocyanine (ZnPc) were purchased from Sigma–Aldrich. Chromatographic purifications were performed on silica gel columns (100–200 mesh, Qingdao Haiyang Chemical Co., Ltd, China) with the indicated eluents. Size-exclusion chromatography was performed on Bio-Rad Bio-Beads S-X3 beads with the indicated eluents. All other solvents and reagents were of reagent grade and used as received.

$^1$H NMR spectra were recorded on a Bruker DPX 300 spectrometer (300 MHz) in $CDCl_3$ or DMSO-$d_6$. Chemical shifts were relative to internal $SiMe_4$ ($\delta = 0$ ppm). Mass spectra were recorded on a Finnigan LCQ Deca xpMAX mass spectrometer. IR spectra were recorded on a Perkin–Elmer SP2000 FT-IR spectrometer, using KBr disks. Elemental analyses were performed by Element Vario EL III equipment. Electronic absorption spectra were measured on a Shimadzu UV-2450 UV–vis spectrophotometer. Fluorescence spectra were taken on an Edinburgh FL900/FS900 spectrofluorometer. Fluorescence quantum yield ($\Phi_F$) and singlet oxygen yield ($\Phi_\Delta$) were determined as described in our previous manuscripts [28].

### 2.2. Synthesis

#### 2.2.1. 3-[2-(4-Boc-piperazine)-1-ethoxy]phthalonitrile (**3a**)

A solution of 1-(2-hydroxyethyl)piperazine (**1a**) (1.4 ml, 10 mmol) in triethylamine (TEA)/$CH_2Cl_2$ (1:5, *v*/*v*, 24 ml) was stirred at room temperature for 10 min, and then di-*tert*-butyl dicarbonate ($Boc_2O$) (2.3 ml, 11 mmol) was added slowly over 10 min. The mixture was further stirred for 12 h. The volatiles were removed under reduced pressure. The oily residue was purified by a silica gel column chromatography using $CH_3OH$ as eluent to give Boc-protected piperazinyl ethanol (Boc = *tert*-butyloxycarbonyl).

Then, a mixture of Boc-protected piperazinyl ethanol (1.15 g, 5.0 mmol), 3-nitrophthalonitrile (**2**) (0.87 g, 5.0 mmol), and anhydrous $K_2CO_3$ (1.38 g, 10 mmol) in DMF (20 ml) was stirred at 40 °C for 48 h. The reaction mixture was poured into ice water (200 ml) to give light red precipitate, which was collected by filtration, washed with water until pH 7 and dried in vacuo. The crude product was purified by recrystallization with DMF/$H_2O$. The oily residue was dissolved in $CHCl_3$, and followed by chromatography on a silica gel column using $CHCl_3$/$CH_3OH$ (10:1, *v*/*v*) as eluent to give a white solid **3a** (1.24 g, 70%). Rf = 0.62 (ethyl acetate). IR (KBr, cm$^{-1}$): 2229 (C≡N); 3077 (Ar-H); 2971, 2869, 1364 ($CH_3$); 2928, 2817 ($CH_2$); 1582, 1473, 1455 (benzene, C=C); 1294, 1283, 1246 (C–O–C, C–N); 1123 (Ar–O–C); 1682.6 (C=O). MS (ESI): *m*/*z* 357.1 $[M + H]^+$. $^1$H NMR (300 MHz, $CDCl_3$, ppm): $\delta = 7.64$ (t, $J = 8.4$ Hz, 1H); 7.36 (d, $J = 7.68$ Hz, 1H); 7.25 (d, $J = 10.4$ Hz, 1H); 4.26 (t, $J = 5.48$ Hz, 2H); 3.43 (t, $J = 4.88$ Hz, 2H); 2.90 (t, $J = 5.46$ Hz, 2H); 2.56 (t, $J = 4.92$ Hz, 2H); 1.46 (s, 9H). Anal. Calcd for $C_{19}H_{24}N_4O_3$: C, 64.03; H, 6.79; N, 15.72. Found C, 63.81; H, 6.71; N, 15.63.

#### 2.2.2. 3-{2-[2-(4-Boc-piperazine)-1-ethoxy]-ethoxy}phthalonitrile (**3b**)

According to the procedure for **3a**, a solution of 1-[2-(2-hydroxyethoxy)ethyl] piperazine (**1b**) (0.86 ml, 5 mmol) in TFA/$CH_2Cl_2$ (1:5, *v*/*v*, 22 ml) was treated with $Boc_2O$ (1.18 ml, 5 mmol) to give Boc-protected piperazinyl ethoxy ethanol. The obtained Boc-protected piperazinyl ethoxy ethanol (1.37 g, 5.0 mmol) was then treated with 3-nitrophthalonitrile (0.87 g, 5.0 mmol) and anhydrous $K_2CO_3$ (1.38 g, 10 mmol) in DMF (20 ml) to give a white solid **3b** (1.13 g, 57%). Rf = 0.59 (ethyl acetate). IR (KBr, cm$^{-1}$): 2226 (C≡N); 3036 (Ar-H); 2976, 2892, 2803, 1472, 1365 ($CH_3$, $CH_2$); 1586, 1472 (benzene, C=C); 1292, 1176, 1131 (C–O–C, C–N); 1247 (Ar–O–C); 1693 (C=O). MS (ESI): *m*/*z* 402.2 $[M + 2H]^+$. $^1$H NMR (300 MHz, $CDCl_3$, ppm): $\delta = 7.62$ (t, $J = 8.4$ Hz, 1H); 7.36 (d, $J = 7.8$ Hz, 1H); 7.28 (d, $J = 8.7$ Hz, 1H); 4.29 (t, $J = 4.6$ Hz, 2H); 3.89 (t, $J = 4.6$ Hz, 2H); 3.72 (t, $J = 5.5$ Hz, 2H); 3.42 (t, $J = 5.0$ Hz, 4H); 2.60 (t, $J = 5.6$ Hz, 2H); 2.43 (t, $J = 5.0$ Hz, 4H); 1.45 (s, 1H). Anal. Calcd for $C_{21}H_{28}N_4O_4$: C, 62.98; H, 7.05; N, 13.99. Found C, 63.25; H, 6.80; N, 14.31.

#### 2.2.3. 1,8(11),15(18),22(25)-tetrakis-[2-(4-Boc-piperazine)-1-ethoxy] phthalocyanine zinc(II) (**4a**)

A suspension of **3a** (0.36 g, 1.0 mmol) in *n*-pentanol (20 ml) was stirred at 90 °C for 10 min, and then anhydrous zinc acetate (0.10 g, 0.54 mmol) and 1,8-diazabicyclo[5.4.0]undec-7-ene (DBU) (0.40 ml, 2.6 mmol) were added. The resulting mixture was stirred at 130 °C for 5 h. After removing the volatiles in vacuo, the residue was purified by a silica gel column chromatography using $CHCl_3$/$CH_3OH$ (18:1, *v*/*v*) as eluent. A green band was collected and concentrated to give a crude product, which was purified by chromatography again using $CHCl_3$/$CH_3OH$ (15:1, *v*/*v*) as eluent. The obtained green solid was further purified by size-exclusion chromatography by using THF as eluent to give a dark-green solid **4a** (0.15 g, 40%). Rf = 0.68 ($CH_3OH$). IR (KBr, cm$^{-1}$): 2970, 2929, 2869, 1365 ($CH_3$, $CH_2$); 1587, 1488 (benzene, C=C); 1175, 1128, 1085 (C–O–C); 1336 (C–N); 1265, 1245 (Ar–O–C); 1697 (C=O); 866, 801, 744 (Ar-H). MS(ESI): *m*/*z* 1488.9$[M]^+$, 1513.7 $[M + Na]^+$. $^1$H NMR (300 MHz, $CDCl_3$, ppm): $\delta = 8.88$–9.03 (m, 4H); 7.69–7.82 (m, 8H); 4.78–4.83 (m, 8H); 3.19–3.28 (m, 16H); 2.67–2.86 (m, 24H); 1.33–1.39 (m, 36H). Anal. Calcd for $C_{76}H_{96}N_{16}O_{12}Zn$: C, 61.22; H, 6.94; N, 15.03. Found: C, 61.56; H, 6.12; N, 15.42.

#### 2.2.4. 1,8(11),15(18),22(25)-tetrakis-{2-[2-(4-Boc-piperazine)-1-ethoxy]-ethoxy} phthalocyanine zinc(II) (**4b**)

According to the above procedure for **4a**, a suspension of **3b** (0.20 g, 0.50 mmol) in *n*-pentanol (10 ml) was treated with anhydrous zinc acetate (0.05 g, 0.27 mmol) and DBU (0.4 ml, 2.6 mmol) to give a dark-green solid **4b** (0.06 g, 33%). Rf = 0.68 ($CH_3OH$). IR (KBr, cm$^{-1}$): 2970, 2927, 2867, 1365 ($CH_3$, $CH_2$); 1588, 1489 (benzene, C=C); 1122, 1082 (C–O–C); 1335 (C–N); 1265, 1245 (Ar–O–C); 1695 (C=O); 866, 801, 745 (Ar-H). MS (ESI): *m*/*z* 1668.7 $[M + H]^+$. $^1$H NMR (300 MHz, $CDCl_3$, ppm): $\delta = 8.99$–9.11 (m, 4H); 7.77–8.17 (m, 8H); 4.16–4.38 (m, 8H); 3.62–3.77 (m, 16H); 3.08 (br, 16H); 2.34 (br, 16H); 2.23 (br, 8H,); 1.19–1.27 (m, 36H). Anal. Calcd for $C_{84}H_{112}N_{16}O_{16}Zn$: C, 60.51; H, 6.77; N, 13.44. Found: C, 61.02; H, 7.15; N, 13.89.

#### 2.2.5. 1,8(11),15(18),22(25)-tetrakis-(2-piperazine-1-ethoxy) phthalocyanine zinc(II) (**5a**)

A solution of phthalocyanine **4a** (0.150 g, 0.10 mmol) in $CH_3OH$ (40 ml) was added with TFA (2.0 ml), and then the mixture was

stirred at room temperature for 30 min. The volatiles were removed in vacuo, and the oily residue was purified by size-exclusion chromatography using THF as eluent to give a dark-green solid **5a** (0.058 g, 53%). IR (KBr, $cm^{-1}$): 2928, 1365 ($CH_2$); 1487, 1457 (benzene, C=C); 1200, 1131 (C–O–C); 1333 (C–N); 1253, 1268 (Ar–O–C); 832, 800, 746 (Ar-H). MS (ESI): *m/z* 1113.4 $[M + Na]^+$. $^1H$ NMR (300 MHz, DMSO-$d_6$, ppm): $\delta = 8.91–9.00$ (m, 4H); 7.71–7.78 (m, 8H); 4.90–4.94 (m, 8H); 4.65–4.70 (m, 8H); 3.78–3.82 (m, 16H); 3.53–3.58 (m, 16H). Anal. Calcd for $C_{56}H_{66}N_{16}O_5Zn$ (**5a**·$H_2O$): C, 60.67; H, 6.00; N, 20.22. Found: C, 60.20; H, 6.34; N, 19.88.

#### 2.2.6. 1,8(11),15(18),22(25)-tetrakis-[2-(2-piperazine-1-ethoxy)-ethoxy]phthalocyanine zinc(II) (**5b**)

According to the procedure for **5a**, phthalocyanine **4b** (0.17 g, 0.10 mmol) in $CH_3OH$ (40 ml) was treated with TFA (2.0 ml) at room temperature for 30 min to give a dark-green solid **5b** (80 mg, 63%). IR (KBr, $cm^{-1}$): 2924 ($CH_2$); 1487, 1477 (benzene, C=C); 1271 (C–O–C); 1326 (C–N); 1271 (Ar–O–C); 3268, 832, 800, 746 (Ar-H); 3424 (tertiary amine). MS (ESI): *m/z* 1302.3 $[M + Cl]^-$. $^1H$ NMR (300 MHz, DMSO-$d_6$, ppm): $\delta = 8.99–9.11$ (m, 4H); 7.77–8.17 (m, 8H); 4.16–4.38 (m, 8H); 3.62–3.77 (m, 16H); 3.08 (br, 16H); 2.34 (br, 16H); 2.23 (br, 8H); 1.19–1.27(m, 4H). Anal. Calcd for $C_{64}H_{82}N_{16}O_9Zn$ (**5b**·$H_2O$): C, 59.83; H, 6.43; N, 17.44. Found: C, 59.87; H, 6.60; N, 17.92.

#### 2.2.7. 1-[2-piperazine-1-ethoxy] phthalocyanine zinc(II) (**7**)

A mixture of phthalonitrile **3a** (0.18 g, 0.50 mmol) and unsubstituted phthalonitrile (**6**) (0.32 g, 2.5 mmol) in *n*-pentanol (20 ml) was stirred at 70 °C for 10 min, and then anhydrous zinc acetate (0.30 g, 1.66 mmol) and DBU (0.4 ml, 2.6 mmol) were added. The resulting mixture was stirred at 130 °C for 12 h. After removing the volatiles in vacuo, the residue was dissolved in $CH_3OH$ (30 ml), and then treated with TFA (30 ml) at room temperature for 30 min. The reaction mixture was poured into ice water (200 ml) to give green precipitate, which was collected by filtration, washed with water until pH 7 and dried in vacuo. The oily residue was purified by a silica gel column chromatography using $CHCl_3/CH_3OH$ (5:1, *v/v*) as eluent to give a blue–green crude, which was further purified by size-exclusion chromatography using THF as eluent to give a blue–green solid **7** (0.019 g, 5%). IR (KBr, $cm^{-1}$): 2957, 2925, 2856, 1365 ($CH_2$); 1608, 1588 (benzene, C=C); 1165, 1092 (C–O–C); 1333 (C–N); 1259 (Ar–O–C); 3056, 885, 800, 772, 751, 736 (Ar-H). MS (ESI): *m/z* 703.1 $[M - H]^-$. $^1H$ NMR (300 MHz, DMSO-$d_6$, ppm): $\delta = 9.39–9.41$ (m, 6H); 9.01–9.03 (m, 1H); 8.23–8.25 (m, 8H); 6.68 (s, 1H); 5.31–5.33 (m, 2H); 4.68–4.69 (m, 2H); 3.32–3.43 (m, 8H). Anal. Calcd for $C_{38}H_{28}N_{10}OZn$: C, 64.64; H, 4.00; N, 19.84. Found: C, 64.19; H, 4.42; N, 20.21.

### 2.3. Oil/water partition coefficients

The oil/water partition coefficients were determined according to the procedure reported by Dei et al. with minor modification [23]. The *n*-octanol (0.5 ml) and phosphate buffered saline (PBS) (0.5 ml) was mixed with $v_{PBS}/v_{octanol}$ (1:1) in a tube, and then about 20 μl of phthalocyanine solution (1 mM in DMF) was added into it. The tube was shaken for 10 min. After that, the separation of the two phases was enabled by centrifugation and the aqueous solution was sampled by using a procedure that minimizes the risk of including traces of *n*-octanol. The phthalocyanine concentration was calculated from the Q-band absorbance in a diluted DMF solution with reference to the corresponding molar absorptivity (see Table 1). The distribution coefficient was then determined by the ratio of phthalocyanine concentration in octanol phase to that in PBS phase. At least three independent measurements were performed and the corresponding $P_{O/W}$ value was taken as the overall average.

### 2.4. Biological studies

#### 2.4.1. Photosensitizer

Stock solutions of the studied zinc phthalocyanines (1 mM) were prepared in *N*,*N*-dimethylformamide (DMF) and stored at 4 °C in the dark. The solution was then diluted to appropriate concentration with PBS (0.01 M, pH 7.4) containing 1% Cremophor EL (1 g, in 100 ml) before use.

#### 2.4.2. Organisms and growth conditions

*Candida albicans* strain CMCC(F)C1a was purchased from Nanjing Institute of Dermatology, Chinese Academy of Sciences. *Candida* cells were plated on Sabouraud dextrose agar and incubated aerobically at 37 °C. After 48 h of incubation, a sample of colonies was removed from the surface of the agar plate and suspended in sterile PBS (0.01 M, pH 7.4). Cells were harvested by centrifugation, and washed with PBS, and re-suspended in PBS to appropriate cell density prior to the experiment.

#### 2.4.3. Photosensitizer uptake by Candida cells

Suspensions of *C. albicans* (0.8 ml, about $2.5 \times 10^7$ cells/ml) in PBS were incubated in dark at 37 °C with 0.1 mM of phthalocyanines for 3 h. The cultures were centrifuged (8000 rpm for 10 min) and the cell pellets were washed with twice PBS, and then re-suspended in 0.8 ml DMF and sonicated for 10 min. The absorption spectrum of the supernatant was measured. The photosensitizer concentration was calculated from the Q-band absorbance in this diluted DMF reference to the corresponding molar absorptivity (see Table 1). Each experiment was repeated 3 times.

#### 2.4.4. In vitro photodynamic inaction of Candida cells in PBS

*Candida* cellular suspensions were incubated with PBS solution containing different concentrations of photosensitizer in a 96-well plate (0.2 ml/well, $2 \times 10^6$ cells/ml), in the dark for 3 h at room temperature. After that, the cultures were exposed to visible light for 30 min. The light source consisted of a 500 W halogen lamp, a water tank for cooling and a color glass filter cut-on 610 nm. The fluence rate ($\lambda > 610$ nm) was 15 mW $cm^{-2}$. An illumination of 30 min led to a total fluence of 27 J $cm^{-2}$. In parallel, three control experiments were designed as follows: (1) with photosensitizer, but non-illuminated, (2) without photosensitizer, but illuminated, (3) no photosensitizer, non-illuminated. Control and irradiated cell suspensions were serially diluted (100-fold) with PBS, and each solution was plated in triplicate onto Sabouraud dextrose agar. After incubation of the plates at 37 °C for 48 h, the number of colonies on each plate was counted. The survival percentage was determined by the comparing the number of colony-forming units with the control (no photosensitizer, non-illuminated). Each experiment was repeated separately 3 times.

#### 2.4.5. Growth delay of C. albicans

The growth delay of *C. albicans* caused by photodynamic actions was determined according to the literature procedure [18]. Suspensions of *C. albicans* (1 ml, about $2 \times 10^6$ cells/ml) in PBS was diluted to 20 ml of fresh Sabouraud broth medium. The suspension was homogenized and aliquots of 0.2 ml were incubated with 25 μM of phthalocyanine **7** in flasks at 37 °C. The flasks were then irradiated with red light ($\lambda > 610$ nm, 15 mW $cm^{-2}$) for 30 min, as described above. The culture grown was measured by turbidity at 492 nm using a MK3 multiskan ascent (Thermo). This wavelength was chosen to avoid the interference of the absorption of phthalocyanines in the range of 300–400 nm and 610–700 nm. In all

cases, control experiments were carried out without illumination in the absence and in the presence of sensitizers. Each experiment was repeated separately 3 times.

## 3. Results and discussion

### 3.1. Synthesis

Scheme 1 shows the synthetic pathway of tetra-substituted phthalocyanines **4a**–**b** and **5a**–**b**. Firstly, the secondary amines on the piperazinyl group of compounds **1a** and **1b** were protected with *tert*-butoxycarbonyl (Boc) group by treating the compound **1a** or **1b** with di-*tert*-butyl dicarbonate in the presence of TEA in $CH_2Cl_2$. The *N*-Boc-protected compounds then underwent nucleophilic substitution with 3-nitrophthalonitrile under alkaline condition to give the corresponding 3-substituted phthalonitriles **3a** and **3b**. The cyclotetramerization of **3a** or **3b** in the presence of zinc acetate and organic base DBU in *n*-pentanol afforded the *N*-Boc-protected tetra-substituted phthalocyanines **4a** and **4b** in 40% and 33% yield, respectively. Subsequently, *N*-Boc-deprotection of these compounds using TFA gave phthalocyanines **5a** and **5b**, respectively.

To demonstrate the effect of the number of substitutes, the mono-substituted zinc(II) phthalocyanine **7** was also prepared using a synthetic route as shown in Scheme 2. The mixed cyclization of *N*-Boc-protected phthalonitrile **3a** with an excess of unsubstituted phthalonitrile (**6**) in the presence of zinc acetate and DBU afforded the *N*-Boc-protected phthalocyanine, which was followed by *N*-Boc-deprotection to afford the targeted phthalocyanine **7**.

All the phthalocyanines have good solubility in common organic solvents, such as DMF, tetrahydrofuran (THF), ethyl acetate, and ethanol. These new compounds were characterized by MS, $^1$H NMR, and FT-IR spectroscopic methods together with elemental analysis.

### 3.2. Photophysical and photochemical properties

The spectroscopic properties of the phthalocyanines **4a**, **4b**, **5a**, **5b**, and **7** were measured in DMF, and the data are summarized in Table 1. The absorption spectra of all compounds in DMF are typical for non-aggregated phthalocyanines, exhibiting an intense and sharp Q-band at 678–700 nm. Fig. S1 (in supporting information) shows the UV–vis spectra of **7** in DMF at various concentrations given as an example. The Q-band strictly followed the Lambert–Beer law, indicating that it is essentially free from aggregation in DMF. Compared with unsubstituted ZnPc, both of the mono- and tetra-substituted phthalocyanines have red-shift Q-band (670 nm vs. 678–700 nm). Furthermore, the Q-band absorption of tetra-substituted phthalocyanines **4a**, **4b**, **5a**, and **5b** (699–700 nm) shows obviously red-shifted compared with that of mono-substituted analog **7** (678 nm). It has been reported that substitution at $\alpha$ position can lead to reduction of the HOMO–LUMO gap, which is consistent with the result of red-shift of these $\alpha$ substituted compounds [29,30]. Upon excitation at 610 nm, the tetra-substituted compounds showed fluorescence emission at 707–709 nm with a Stokes shift of ca. 9 nm. Their fluorescence

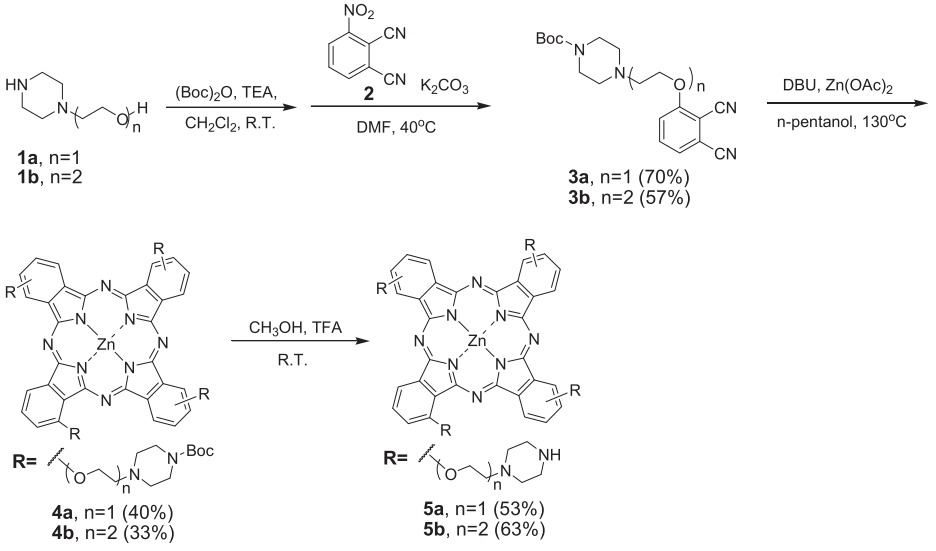


**Scheme 1.** Synthesis of tetra-substituted zinc(II) phthalocyanines **4**–**5a** and **4**–**5b**.

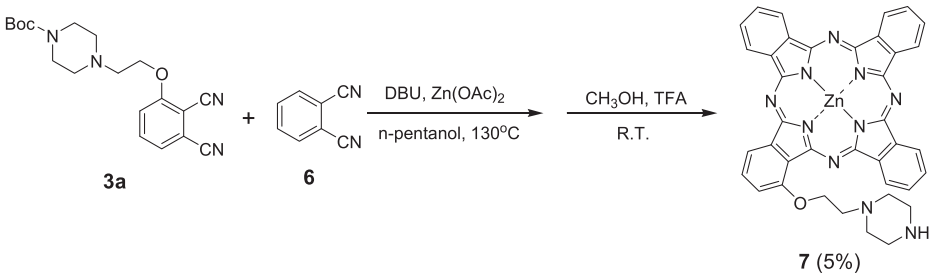


**Scheme 2.** Synthesis of mono-substituted phthalocyanine **7**.

**Table 1**
Photophysical and photochemical data for phthalocyanines in DMF.

| Phthalocyanines | $\lambda_{max}$ (nm) | $\lambda_{em}$ (nm)[a] | Stokes shift (nm) | $\varepsilon \times 10^5$ ($M^{-1}$ $cm^{-1}$) | $\Phi_F$[b] | $\Phi_\Delta$[c] |
|---|---|---|---|---|---|---|
| **4a** | 700 | 709 | 9 | 1.73 | 0.12 | 0.64 |
| **4b** | 699 | 707 | 8 | 1.76 | 0.13 | 0.77 |
| **5a** | 700 | 709 | 9 | 1.08 | 0.11 | 0.56 |
| **5b** | 700 | 708 | 8 | 1.14 | 0.11 | 0.69 |
| **7** | 678 | 680 | 2 | 1.77 | 0.27 | 0.54 |

[a] Excited at 610 nm.
[b] Using unsubstituted zinc(II) phthalocyanine (ZnPc) in DMF as the reference ($\Phi_F = 0.28$) [31].
[c] Determined using DPBF as chemical quencher, and using ZnPc in DMF as the reference ($\Phi_\Delta = 0.56$) [32,33].

quantum yields ($\Phi_F = 0.11$–$0.13$) are obviously lower than that of ZnPc ($\Phi_F = 0.28$) [31]. For the mono-substituted analog **7**, the fluorescence emission was at 680 nm with a comparable fluorescence quantum yield ($\Phi_F = 0.27$) with that of ZnPc. This is in accord with the general observation that the lower the energy of the Q-band, the smaller the $\Phi_F$ value [29,30].

The singlet oxygen quantum yields ($\Phi_\Delta$) of these compounds were also determined in DMF by a steady-state method by using 1,3-diphenylisobenzofuran (DPBF) as the scavenger [32,33]. As shown in Table 1, all the compounds are efficient singlet oxygen generators with $\Phi_\Delta$ of 0.54–0.77, which suggests that the singlet oxygen generation efficiency of zinc(II) phthalocyanines are not quenched significantly by the amine of the piperazinyl moiety. However, it has been reported that, for silicon(IV) phthalocyanines, both their fluorescence and singlet oxygen generation efficiency are badly quenched by amino moieties through photoinduced electron effect (PET), which leads to the obvious reduction of photodynamic activities of these compounds [27,34]. On the other hand, the phthalocyanines **4b** and **5b** containing longer ethoxy chain between macrocycle and piperazinyl moiety can generate singlet oxygen more efficiently than their counterparts **4a** and **5a**, respectively ($\Phi_\Delta = 0.77$ for **4b** vs.0.64 for **4a**, and 0.69 for **5b** vs. 0.56 for **5a**).

Aggregation behavior of photosensitizers will reduce their photosensitizing efficiencies. Therefore, the aggregation trends of these compounds were also examined in aqueous solutions by absorption spectroscopic method. Fig. 1 shows the UV–vis spectra of tetra-substituted **5a** and mono-substituted **7** as examples. They show very broad and weak Q-band at approximately 705 nm and 685 nm in water with 0.5% DMF, which means they are significantly aggregated in water. However, in the presence of a tiny amount of Cremophor EL, which is a non-ionic surfactant usually used as a formulation vehicle of hydrophobic drugs [35], the Q-band is basically intense and sharp similar to that in DMF. Similar results were observed for the other counterparts **4a**, **4b**, and **5b**. Furthermore, the absorbance at different concentrations was also measured in the aqueous (Fig. 2, **7** is given as an example). The absorption well obeys the Lambert–Beer law, suggesting that aggregation is not significant for these phthalocyanines when formulated with Cremophor EL in the aqueous solution.

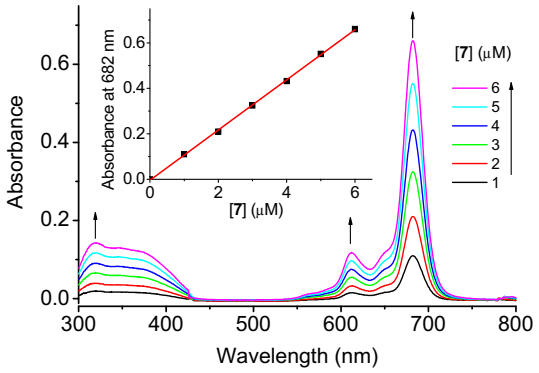


**Fig. 2.** UV–vis spectra of phthalocyanine **7** at different concentrations in $H_2O$ containing 1% Cremophor EL. The inset shows the plot of the Q-band absorbance against the concentration.

### 3.3. In vitro antifungal studies

The in vitro photodynamic antifungal activities of these compounds **4a**, **4b**, **5a**, **5b**, and **7** formulated with Cremophor EL were firstly investigated against *C. albicans*. The cells were incubated with these photosensitizers at different concentrations in the dark at room temperature for 3 h. After that, the cells were irradiated with red light, and then the viable cells were determined. Fig. 3 shows the dose-dependent survival curves in the absence and presence of light. It is clear that all the compounds are essentially noncytotoxic in dark. Their curves in dark are similar with that of the control, in which the culture was incubated without sensitizer just illuminated with the red light. In the presence of light, the photocytotoxicities of these compounds follow the trend: **7** > **5a** > **5b** > **4a** ≈ **4b**. The *N*-Boc-protected **4a** and **4b** are basically noncytotoxic against the cells until 100 μM upon illumination (Fig. 3a). For the tetra-substituted **5a** and **5b**, the compound **5a** containing shorter ethoxy chain shows higher photocytotoxicity than the analog **5b**. For all the compounds, the mono-substituted **7** presents the highest photocytotoxicity with an $IC_{90}$ value as low as 9 μM.

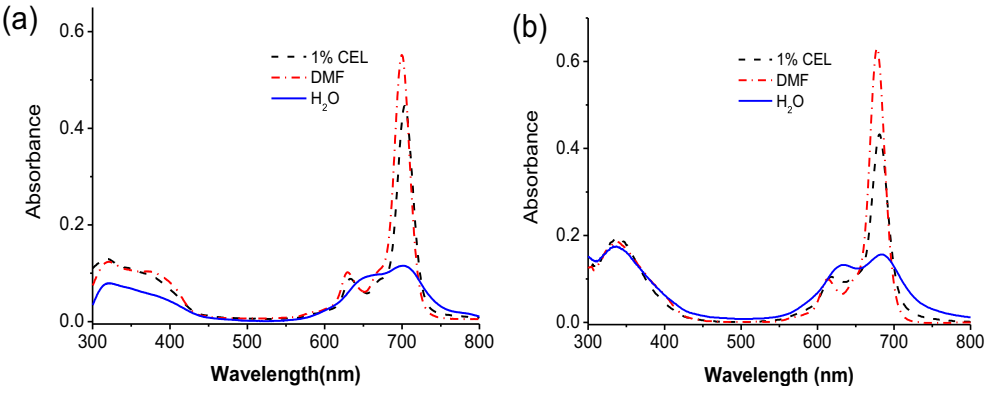


**Fig. 1.** UV–vis spectra of (a) **5a** and (b) **7** in 1% CEL (—), DMF (- -), and water (with 0.5% DMF) (—) (All at 4 μM). 1% CEL: 1% Cremophor EL in water (1 g in 100 mL of water).

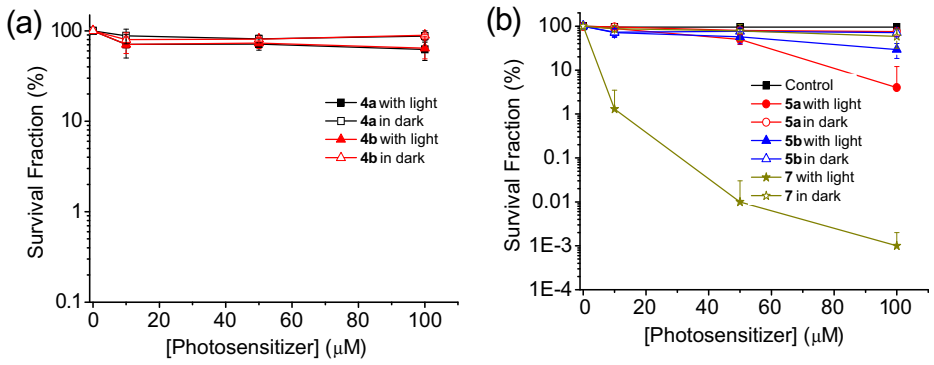


**Fig. 3.** Photocytotoxic effects of (a) **4a**–**b**, and (b) **5a**–**b** and **7** on *C. albicans* in the absence and presence of red light ($\lambda > 610$ nm) at a dose of 27 J cm$^{-2}$. Control means the culture was incubated without sensitizer and kept illumination as above. Values represent as the mean ± standard deviation of three separate experiments. (For interpretation of the references to colour in this figure legend, the reader is referred to the web version of this article.)

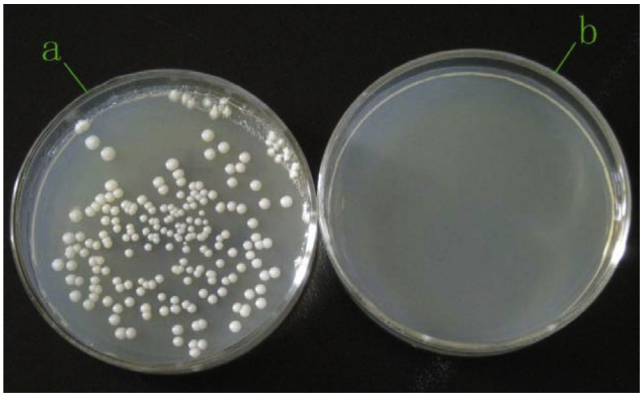


**Fig. 4.** The photodynamic activity of phthalocyanine **7** against *C. albicans*. (a) control (without **7**) (b) incubation with **7** (50 μM) for 3 h, followed by irradiation with red light ($\lambda > 610$ nm) at a dose of 27 J cm$^{-2}$.

Methylene Blue (MB), a known antifungal photosensitizer [11,12], has been selected as a positive control in this assay. Under the same experimental condition, the $IC_{90}$ value of MB against *C. albicans* cells was found to be ca. 500 μM, which is about 50 times higher than that of phthalocyanine **7**. Clearly, compound **7** exhibits a much higher photocytotoxicity against *C. albicans* than MB, suggesting that **7** is a potential photosensitizer for antifungal photodynamic therapy.

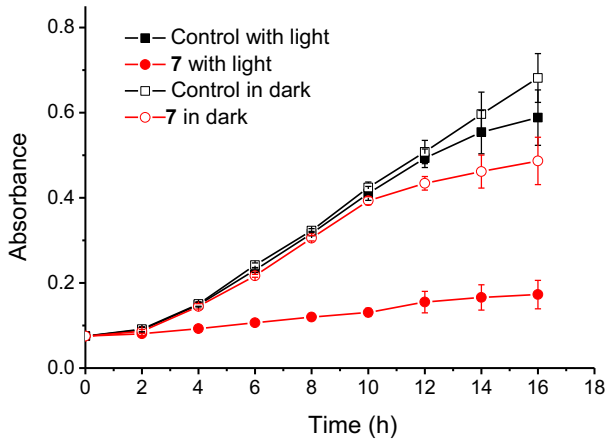


**Fig. 5.** Growth delay curves of *C. albicans* cells incubated with phthalocyanine **7** (25 μM) upon illumination with red light (>610 nm) at a dose of 27 J cm$^{-2}$. Control cultures were incubated without sensitizer in the absence or presence of light. Values represent as the mean ± standard deviation of three independent experiments. (For interpretation of the references to colour in this figure legend, the reader is referred to the web version of this article.)

The photodynamic antifungal activity of **7** can also be observed from Fig. 4. The *C. albicans* cells were virtually killed for the dish incubated with **7** (50 μM) for 3 h upon illumination, while for the dish without **7**, a large amount of *C. albicans* was found.

To ensure that photodynamic inactivation of fungal cells is still maintained when the cultures were not under starvation conditions, growth delay of *C. albicans* sensitized by phthalocyanine **7** was further carried out in Sabouraud medium. The cell growth of the *C. albicans* was examined under four conditions, containing in the absence or presence of phthalocyanine **7** (25 μM), and with or without illumination. As shown in Fig. 5, when the *C. albicans* cultures were treated with phthalocyanine **7** upon illumination, cell growth of the *C. albicans* can be suppressed efficiently in the following 16 h. On the other hand, the *C. albicans* cells incubated with phthalocyanine **7** in dark shows no significant growth delay, which is comparable with the controls. The result indicates that the observed growth delay can be ascribed to the photodynamic effect of the sensitizers on the cells.

To account for the different photocytotoxic results of these compounds, the cellular uptake was also investigated by an extraction method. As shown in Table 2, the cellular uptake of these compounds follows the trend **7** > **5a** ≈ **5b** > **4a** ≈ **4b**. The cellular uptake of **7** is significantly higher than all the other compounds. The compounds **5a** and **5b** present higher cellular uptake compared to the corresponding *N*-Boc-protected **4a** and **4b**. Therefore, the trend in cellular uptake of these phthalocyanines is generally in accord with the observed result of photoactivity toward *Candida* cells (**7** > **5a** > **5b** > **4a** ≈ **4b**). This indicates that the different photodynamic activity against *C. albicans* of these compounds is largely attributed to the differences in cellular uptake.

To understand further the different cellular uptakes of these compounds, we examined their hydrophilic–hydrophobic characteristics by measuring the octanol/PBS partition coefficient ($P_{O/W}$). The Log $P_{O/W}$ values were summarized in Table 2. The Log $P_{O/W}$ values follow the order: **4a** > **4b** > **7** > **5a** > **5b**. Compared to Boc-protected

**Table 2**
Partition coefficients and cellular uptakes of phthalocyanines.

| Phthalocyanine | **4a** | **4b** | **5a** | **5b** | **7** |
|---|---|---|---|---|---|
| Log $P_{O/W}$ | 2.05 | 1.81 | 1.34 | 0.68 | 1.77 |
| [a]Uptake (%) | 0.78 ± 0.03 | 0.94 ± 0.03 | 1.47 ± 0.16 | 1.85 ± 0.28 | 4.54 ± 0.14 |

[a] Percentages of cellular uptake of phthalocyanines by *C. albicans* after 3 h incubation. Values represent as the mean ± standard deviation of three independent experiments.

compounds **4a** and **4b**, the corresponding Boc-deprotected analogs **5a** and **5b** show lower Log $P_{O/W}$ values, which can be due to the lipophilic *t*-butyl moieties of the Boc groups on the **4a** and **4b**. The phthalocyanines **4b** and **5b** substituted with longer ethoxy chains have lower Log $P_{O/W}$ value relative to their analogs **4a** and **5a**, respectively, which indicates that the elongation of ethoxy chain can enhance the hydrophilicity. The Log $P_{O/W}$ value of the mono-substituted phthalocyanine **7** is higher than the corresponding tetra-substituted analog **5a**. Compared with the other compounds, the mono-substituted phthalocyanine **7** shows a better amphiphilicity. This may account for its higher cellular uptake by *C. albicans* than the other compounds.

## 4. Conclusions

We have prepared and characterized a series of zinc(II) phthalocyanines tetra-substituted or mono-substituted with piperazinyl moieties, which are favorable for the cellular uptake of fungal cells. The structure–activity relationship of these phthalocyanines has been discussed by combination of their photophysical and photochemical properties, cellular uptakes and in vitro photodynamic antifungal activities. The mono-substituted phthalocyanine **7** presents the highest photodynamic activity against *C. albicans* as a result of better amphiphilicity and higher cellular uptake. The $IC_{90}$ value of **7** is down to 9 μM. The results indicate that the mono-substituted zinc(II) phthalocyanine **7** is a promising photosensitizer for antifungal PDT.

## Acknowledgments

This work was supported by the Natural Science Foundation of China (Grant Nos. 20872016, 21172037), the Natural Science Foundation of Fujian, China (Grant No. 2011J01040), and Specialized Research Fund for the Doctoral Program of Higher Education (Grant No. 201135141001).

## Appendix A. Supplementary data

Supplementary data related to this article can be found at http://dx.doi.org/10.1016/j.dyepig.2013.04.032.

## References

[1] Dougherty T, Gomer C, Henderson B, Jori G, Kessel D, Korbelik M, et al. Photodynamic therapy. J Natl Cancer Inst 1998;90:889–905.
[2] Dolmans DEJGJ, Fukumura D, Jain RK. Photodynamic therapy for cancer. Nat Rev Cancer 2003;3:380–7.
[3] Brown SB, Brown EA, Walker I. The present and future role of photodynamic therapy in cancer treatment. Lancet Oncol 2004;5:497–508.
[4] Celli JP, Spring BQ, Rizvi I, Evans CL, Samkoe KS, Verma S, et al. Imaging and photodynamic therapy: mechanisms, monitoring, and optimization. Chem Rev 2010;110:2795–838.
[5] Tardivoa JP, Giglio AD, Oliveirab CS, Gabrielli DS, Junqueira HC, Tada DB, et al. Methylene blue in photodynamic therapy: from basic mechanisms to clinical applications. Photodiagn Photodyn Ther 2005;2:175–91.
[6] Lyon JP, Azevedo CS, Moreira LM, Lima CJ, Resende MA. Photodynamic antifungal therapy against Chromoblastomycosis. Mycopathologia 2011;172:293–7.
[7] Wainwright M. Photodynamic antimicrobial chemotherapy. J Antimicrobiol 1998;42:13–28.
[8] Lyon JP, Moreira LM, Moraes PCG, Santos FV, Resende MA. Photodynamic therapy for pathogenic fungi. Mycoses 2011;54:265–71.
[9] Donnelly RF, McCarron PA, Tunney MM. Antifungal photodynamic therapy. Microbiol Res 2008;163:1–12.
[10] Jori G, Fabris C, Soncin M, Ferro S, Coppellotti O, Dei D, et al. Photodynamic therapy in the treatment of microbial infections: basic principles and perspective applications. Lasers Surg Med 2006;38:468–81.
[11] Espinel-Ingroff A. Novel antifungal agents, targets or therapeutic strategies for the treatment of invasive fungal diseases: a review of the literature (2005–2009). Rev Iberoam Micol 2009;26:15–22.
[12] Giroldo LM, Felipe MP, Oliveira MA, Munin E, Alves LP, Costa MS. Photodynamic antimicrobial chemotherapy (PACT) with methylene blue increases membrane permeability in *Candida albicans*. Lasers Med Sci 2009;24:109–12.
[13] Oriel S, Nitzan Y. Photoinactivation of *Candida albicans* by its own endogenous porphyrins. Curr Microbiol 2010;60:117–23.
[14] Rex JH, Rinaldi MG, Pfaller MA. Resistance of *Candida* species to fluconazole. Antimicrob Agents Chemother 1995;39:1–8.
[15] Goldman GH, Savoldi M, Perlin D, Savoldi M, Perlin D, Park S, et al. Evaluation of fluconazole resistance mechanisms in *Candida albicans* clinical isolates from HIV-infected patients in Brazil. Diagn Microbe Infec Dis 2004;50:25–32.
[16] Donnelly RF, McCarron PA, Tunney MM, Woolfson A. Potential of photodynamic therapy in treatment of fungal infections of the mouth. Design and characterisation of a mucoadhesive patch containing toluidine blue O. J Photochem Photobiol B 2007;86:59–69.
[17] Munina E, Giroldo LM, Alves LP, Costa MS. Study of germ tube formation by *Candida albicans* after photodynamic antimicrobial chemotherapy (PACT). J Photochem Photobiol B 2007;88:16–20.
[18] Cormick M, Alvarez MG, Rovera M, Durantini EN. Photodynamic inactivation of *Candida albicans* sensitized by tri- and tetra-cationic porphyrin derivatives. Eur J Med Chem 2009;44:1592–9.
[19] Lambrechts SAG, Aalders MCG, Verbraak FD, Lagerberg JWM, Dankert JB, Schuitmaker JJ. Effect of albumin on the photodynamic inactivation of microorganisms by a cationic porphyrin. J Photochem Photobiol B 2005;79:51–7.
[20] Nyokong T. Effects of substituents on the photochemical and photophysical properties of main group metal phthalocyanines. Coord Chem Rev 2007;251:1707–22.
[21] Wainwright M. Photodynamic therapy: the development of new photosensitisers. Anticancer Agents Med Chem 2008;8(3):280–91.
[22] Cosimelli B, Roncucci G, Dei D, Fantetti L, Ferroni F, Ricci M, et al. Synthesis and antimycotic activity of new unsymmetrical substituted zinc phthalocyanines. Tetrahedron 2003;59:10025–30.
[23] Dei D, Chiti G, Filippis MP, Fantetti L, Giuliani F, Giuntini F, et al. Phthalocyanines as photodynamic agents for the inactivation of microbial pathogens. J Porphyrins Phthalocyanines 2006;10:147–59.
[24] Mantareva V, Kussovski V, Angelov I, Borisova E, Avramov L, Schnurpfeil G, et al. Photodynamic activity of water-soluble phthalocyanine zinc(II) complexes against pathogenic microorganisms. Bioorg Med Chem 2007;15:4829–35.
[25] So CW, Tsang PW, Lo PC, Seneviratne CJ, Samaranayake LP, Fong WP. Photodynamic inactivation of *Candida albicans* by BAM-SiPc. Mycoses 2009;53:215–20.
[26] Lam M, Jou PC, Lattif AA, Lee Y, Malbasa CL, Mukherjee PK, et al. Photodynamic therapy with Pc4 induces apoptosis of *Candida albicans*. Photochem Photobiol 2011;87:904–9.
[27] Zheng BY, Lin T, Yang HH, Huang JD. Photodynamic inactivation of *Candida albicans* sensitized by a series of novel axially di-substituted silicon (IV) phthalocyanines. Dyes Pigments 2013;96:547–53.
[28] Shen XM, Jiang XJ, Huang CC, Huang JD. Highly photostable silicon (IV) phthalocyanines containing adamantane moieties: synthesis, structure, and properties. Tetrahedron 2010;66:9041–8.
[29] Kobayashi N, Sasaki N, Higashi Y, Osa T. Regiospecific and nonlinear substituent effects on the electronic and fluorescence spectra of phthalocyanines. Inorg Chem 1995;34:1636–7.
[30] Kobayashi N, Ogata H, Nonaka N, Luk'yanets EA. Effect of peripheral substitution on the electronic absorption and fluorescence spectra of metal-free and zinc phthalocyanines. Chem Eur J 2003;9:5123–34.
[31] Scalise I, Durantini EN. Synthesis, properties, and photodynamic inactivation of *Escherichia coli* using a cationic and a noncharged Zn(II) pyridyloxyphthalocyanine derivatives. Bioorg Med Chem 2005;13:3037–45.
[32] Maree MD, Kuznetsova N, Nyokong T. Silicon octaphenoxyphthalocyanines: photostability and singlet oxygen quantum yields. J Photochem Photobiol A 2001;140:117–25.
[33] Spiller W, Kliesch H, Wohrle D, Hackbarth S, Roder B, Schnurpfeil G. Singlet oxygen quantum yields of different photosensitizers in polar solvents and micellar solutions. J Porphyrins Phthalocyanines 1998;2:145–8.
[34] Jiang XJ, Lo PC, Yeung SL, Fong WP, Ng DKP. Phthalocyanine-polyamine conjugates as highly efficient photosensitizers for photodynamic therapy. J Med Chem 2011;54:320–30. and references cited therein.
[35] Gelderblom H, Verweij J, Nooter K, Sparreboom A, Cremophor EL. the drawbacks and advantages of vehicle selection for drug formulation. Eur J Can 2001;37:1590–8. and references cited therein.